International Journal of Science and Research (IJSR)
ISSN: 2319-7064
Impact Factor 2025: 7.089

XRD Characteristics as an Indicator of Mechanical Strength in Biodegradable Alloys

Rajnish Kumar Bharati[1], Rina Sahu[2]

[1]Department of Metallurgical and Materials Engineering, National Institute of Technology, Jamshedpur, 831014, India
Corresponding Author Email: *rkb.stmary[at]gmail.com*
ORCID ID: 0009-0003-5069-4485

[2]Department of Metallurgical and Materials Engineering, National Institute of Technology, Jamshedpur, 831014, India

Abstract: ***The optical micrograph (OM) and X-ray diffraction (XRD) are examined in this work. The findings verify that all alloys contain α-Mg with $MgZn_2$ secondary phases. Limited strengthening is indicated by the base Mg-5Zn alloy's larger crystallite size (8.27–25.62), lower lattice strain, and coarser grains (~99 µm). The microstructure and strength capacity are greatly improved by alloying additions. The Ca-containing alloy has better structural stability and moderate grain refinement (~93 µm). Defect strengthening is aided by the addition of Mn, which increases dislocation density and decreases grain size (~89 µm). The alloy is containing Sr exhibits the smallest grain size (~76 µm), largest lattice strain, finest crystallite size (7.79-12.62 nm), and greater precipitate volume. Overall, microstructural refinement and defect density increase in the order Mg-5Zn < Mg-5Zn-0.3Ca < Mg-5Zn-0.3Mn < Mg-5Zn-0.3Sr, with Sr providing the most effective strengthening for biodegradable Mg–Zn alloys.***

Keywords: Crystalline Size, Lattice Strain, Dislocation Density

Research Highlight
Among all compositions, Mg–5Zn–0.3Sr exhibits the highest strengthening effect due to the combined contribution of grain refinement, lattice distortion, and increased precipitate formation.

Graphical Abstract

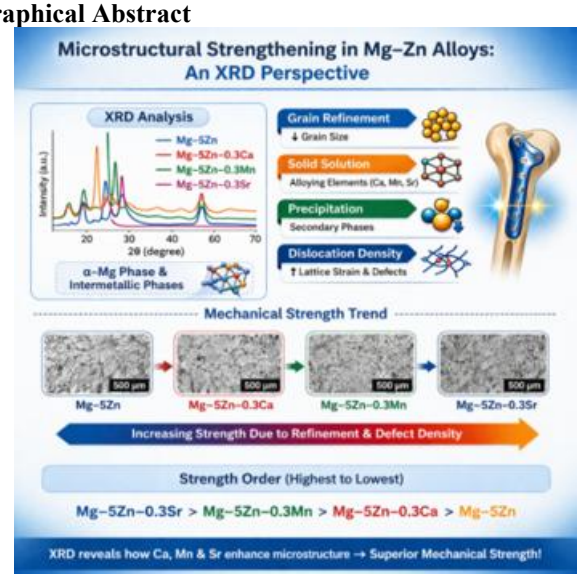

1. Introduction

Metallic biomaterials are widely utilized in orthopedic applications due to their high strength and fracture toughness, making them more reliable than polymers and ceramics for load-bearing conditions [1]. Magnesium (Mg) has emerged as a promising biodegradable implant material owing to its excellent biocompatibility and mechanical compatibility with natural bone [2]. Mg is an essential element in the human body, playing a vital role in bone metabolism and cellular functions, with nearly 50-60% stored in bone tissues [3-5]. X-ray diffraction (XRD) is an effective tool for evaluating the crystal structure and microstructural parameters of Mg-based alloys. In this study, Mg-5Zn and its Ca, Mn, and Sr modified alloys were analysed using XRD data such as diffraction angle (2θ), interplanar spacing (d), and full width at half maximum (β). The crystallite size (D) was calculated using the Scherrer equation: $D = K*\lambda/(\beta*cos\theta)$ (Eq. 1) Where, D is the crystallite size (nm), K is the shape factor (~0.9), λ is the X-ray wavelength (Å), β is the FWHM and θ is the Bragg angle [6]. This relation indicates that D is inversely proportional to β, implying that peak broadening leads to crystallite refinement and increased strength via grain boundary strengthening. Lattice strain (ε) was estimated using: $\varepsilon = \beta/(4*tan\theta)$ (Eq. 2) Where, ε represents microstrain (10^{-3}). Increased strain reflects lattice distortion due to atomic size mismatch and contributes to strengthening by restricting dislocation motion [7]. Dislocation density (δ) was calculated as: $\delta = 1/D^2$ (Eq. 3) Where, δ (m^{-2}) indicates defect density. Higher dislocation density enhances strength by impeding plastic deformation [8]. The addition of Ca, Mn, and Sr introduces crystalline size, lattice strain and dislocation density as well as promotes secondary phase formation. These effects collectively refine the microstructure and enhance mechanical strength, demonstrating the importance of XRD derived parameters in understanding and optimizing Mg-Zn based biodegradable alloys for biomedical applications.

2. Materials and Methods

High-purity Mg (99.9 wt%) and Zn were used to prepare the Mg–5Zn base alloy. Alloying elements Ca, Mn, and Sr (0.3 wt% each) were introduced using Mg–20Ca, Mg–10Mn, and Mg–20Sr master alloys to produce Mg-5Zn-0.3Ca, Mg-5Zn-0.3Mn, and Mg–5Zn–0.3Sr compositions. Melting was carried out in an electric resistance furnace at 760 °C under an argon atmosphere to prevent oxidation. A flux mixture of $MgCl_2$, NaCl, MgO, and CaF_2 was used during melting. The molten alloy was stirred to ensure homogeneity, followed by slag removal and casting into preheated $CaCO_3$-coated steel

moulds. X-ray diffraction (XRD) analysis was performed using a Rigaku ULTIMA IV Diffractometer with Cu Kα radiation (40 kV, 20 mA), scanned over a 20°-90° range at 1°/min. Optical Micrograph (OM) analysis was conducted using a Leica DFC295 metallurgical microscope.

3. Results and Discussion

3.1 Mg-5Zn alloy

The XRD pattern (Figure 1) limited secondary phase formation and confirms the presence of α-Mg as the dominant phase along with minor $MgZn_2$ intermetallics. According to the computed data, the crystallite size (Table 1) ranges from 8.27 to 25.62, with an average tendency toward larger values. Accordingly, the dislocation density (Table 1) stays relatively low (0.0015-0.0146) and the lattice strain (Table 1) varies from 0.0428 to 0.1176. This suggests a crystal lattice with fewer defects and less distortion. The OM (Figure 2) further reveals the moderate precipitate volume (~6.226) and comparatively coarser grains (99±16.06) as shown in table 2. Because of its larger crystallite size, lower lattice strain, and lower dislocation density, Mg–5Zn shows a lower strengthening contribution.

3.2 Mg-5Zn-0.3Ca Alloy

Peak broadening and intensity are showing in (Figure 1) change noticeably when Ca is added, suggesting increased lattice distortion and grain refinement. Strengthening is aided by the presence of $MgZn_2$ and Ca-containing phases (Mg_xCa_y). In comparison to Mg-5Zn, the crystallite size (Table 1) is smaller, ranging from about 8.95 to 17.27, indicating a general decrease. Heterogeneous lattice distortion (Table 1) is suggested by the lattice strain (Table 1) increasing at some peaks (~0.0673) while decreasing at others (as low as 0.0067). The values of dislocation density (0.0003–0.0124) are moderate. Grain refinement (Table 2) caused by Ca addition is confirmed by the reduction in grain size to 93±13.56. Through the Hall-Petch mechanism, this refinement increases strength. The precipitate volume (~6.012%) (Table 2), is still similar to the base alloy, though, suggesting that grain refinement rather than precipitation hardening is the primary cause of strengthening.

3.3 Mg–5Zn–0.3Mn Alloy

Refined crystallites and a higher defect density are indicated by the Mn-containing alloy's notable peak intensity increase and slight peak broadening. The XRD results show in (Fig. 1) that Mn is known to enhance solid solution strengthening and impurity control. Strengthening is also aided by the presence of $MgZn_2$ and Mn-containing phases (Mg_xMn_y). The crystallite size (Table 1) exhibits refinement in comparison to the base alloy, ranging from approximately 8.71 to 16.25. Moderate lattice distortion (Table 1) is indicated by the lattice strain, which ranges from 0.0377 to 0.1022. Increased defect concentration (Table 1) is confirmed by the comparatively higher dislocation density (0.0037–0.0131). With the lowest precipitate volume (~5.002%) (Table 2) of all the alloys, the OM (Figure 2) reveals additional grain refinement to ~89±13.86 µm. This implies that dislocation strengthening and grain refinement, as opposed to precipitate strengthening, dominate strengthening.

3.4 Mg–5Zn–0.3Sr Alloy

The alloy containing Sr exhibits the strongest peak broadening as shown in Figure 1, which is indicative of the finest crystallite structure and maximum lattice distortion. Strengthening is greatly aided by the formation of $MgZn_2$ and Sr-containing intermetallic phases (Mg_xSr_y). The crystallite size (Table 1), which ranges about 7.79-12.62, is the smallest of all the alloys. Both the dislocation density (Table 1) (0.0062–0.0164) and the lattice strain (Table 1) (0.0753–0.1019) are relatively high. This unmistakably shows a lattice that is severely distorted and has a high defect density. The OM (Figure 2, Table 2) verifies the highest precipitate volume (~6.410%) and the finest grain structure (~76±30 µm). This combination points to significant contributions from dislocation strengthening, precipitation strengthening, and grain refinement.

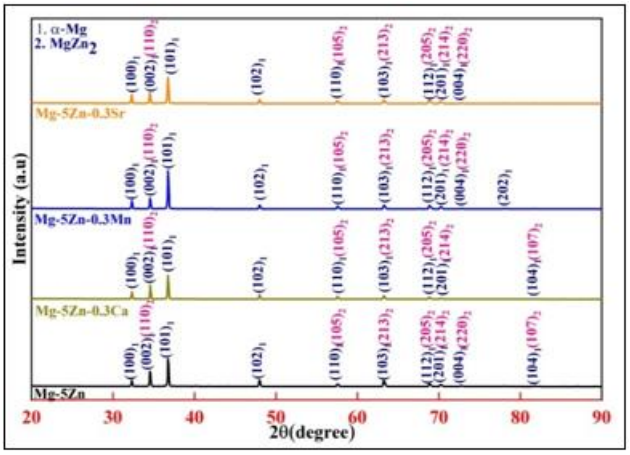

Figure 1: XRD patterns of alloys Mg-5Zn, Mg-5Zn-0.3Ca, Mg-5Zn-0.3Mn, Mg-5Zn-0.3Sr

Table 1: XRD peak parameters are of Mg-5Zn, Mg-5Zn-0.3Ca, Mg-5Zn-0.3Mn and Mg-5Zn-0.3Sr alloys.

Alloys	*2θ*	*I*	*d*	*β*	*β*Cosθ*	*D*	*4*Tanθ*	*ε*	*δ*
Mg-5Zn	32.25	106112.6	2.77161	0.136	0.13064	10.608	1.1564	0.1176	0.0088
	34.45	288262.7	2.59683	0.1178	0.11251	12.318	1.2401	0.0949	0.0069
	36.77	391257.6	2.44751	0.057	0.05409	25.623	1.3294	0.0428	0.0015
	47.95	114626.3	1.89764	0.1408	0.12865	10.773	1.7788	0.0791	0.0086
	57.55	46386.18	1.60179	0.1911	0.16750	8.274	2.1967	0.0869	0.0146
	63.28	123601.9	1.47129	0.1116	0.09501	14.587	2.4646	0.0452	0.0046
	68.84	37926.82	1.36491	0.1183	0.09758	14.202	2.7409	0.0431	0.0049
	70.18	26740.61	1.34141	0.1249	0.10219	13.561	2.8102	0.0444	0.0054
Mg-5Zn-0.3Ca	32.25	144582	2.77161	0.0885	0.08501	16.302	1.1564	0.0765	0.0037
	34.45	266464.8	2.59537	0.0084	0.00802	172.74	1.2401	0.0067	0.0003

	36.77	451434	2.44622	0.1152	0.10932	12.678	1.3294	0.0866	0.0062
	47.95	85582.25	1.8969	0.1158	0.10580	13.099	1.7788	0.0650	0.0058
	57.55	54377.16	1.60179	0.1417	0.12420	11.159	2.1967	0.0645	0.0080
	63.28	68455.77	1.47045	0.1531	0.13034	10.633	2.4646	0.0621	0.0088
	68.84	39633.51	1.36422	0.1756	0.14485	9.568	2.7409	0.0640	0.0109
	70.18	20488.4	1.34074	0.1893	0.15489	8.948	2.8102	0.0673	0.0124
Mg-5Zn-0.3Mn	32.25	156600.3	2.76995	0.1183	0.11364	12.195	1.1564	0.1022	0.0067
	34.45	207850	2.59683	0.1101	0.10516	13.179	1.2401	0.0887	0.0057
	36.77	723783.4	2.44622	0.1114	0.10571	13.110	1.3294	0.0837	0.0058
	47.95	76591.53	1.89615	0.1405	0.12837	10.796	1.7788	0.0789	0.0085
	57.55	56863.77	1.60179	0.1727	0.15137	9.1561	2.1967	0.0786	0.0119
	63.28	72474.61	1.47003	0.1869	0.15911	8.7104	2.4646	0.0758	0.0131
	68.84	47788.66	1.36491	0.1034	0.08529	16.249	2.7409	0.0377	0.0037
	70.18	46506.49	1.34008	0.1714	0.14024	9.882	2.8102	0.0609	0.0102
Mg-5Zn-0.3Sr	32.25	167033	2.77161	0.1179	0.11326	12.237	1.1564	0.1019	0.0066
	34.45	200920.9	2.59975	0.115	0.10984	12.618	1.2401	0.0927	0.0062
	36.77	508689	2.44622	0.1292	0.12260	11.304	1.3294	0.0971	0.0078
	47.95	76802.66	1.8969	0.1407	0.12856	10.780	1.7788	0.0790	0.0086
	57.55	58167.51	1.60286	0.1785	0.15645	8.858	2.1967	0.0812	0.0127
	63.28	66785.58	1.47087	0.1907	0.16235	8.536	2.4646	0.0773	0.0137
	68.84	64360.08	1.36422	0.2064	0.17026	8.140	2.7409	0.0753	0.0150
	70.18	40026.85	1.34141	0.2173	0.17780	7.795	2.8102	0.0773	0.0164

Table 2: Grain Size and Volume of Precipitation of Mg-based alloys

Alloys	Grain Size	Volume of precipitate
Mg-5Zn	99 ± 16.06	6.226 ± 1.09
Mg-5Zn-0.3Ca	93 ± 13.56	6.012 ± 3.41
Mg-5Zn-0.3Mn	89 ± 13.86	5.002 ± 1.03
Mg-5Zn-0.3Sr	76 ± 30.00	6.410 ± 0.45

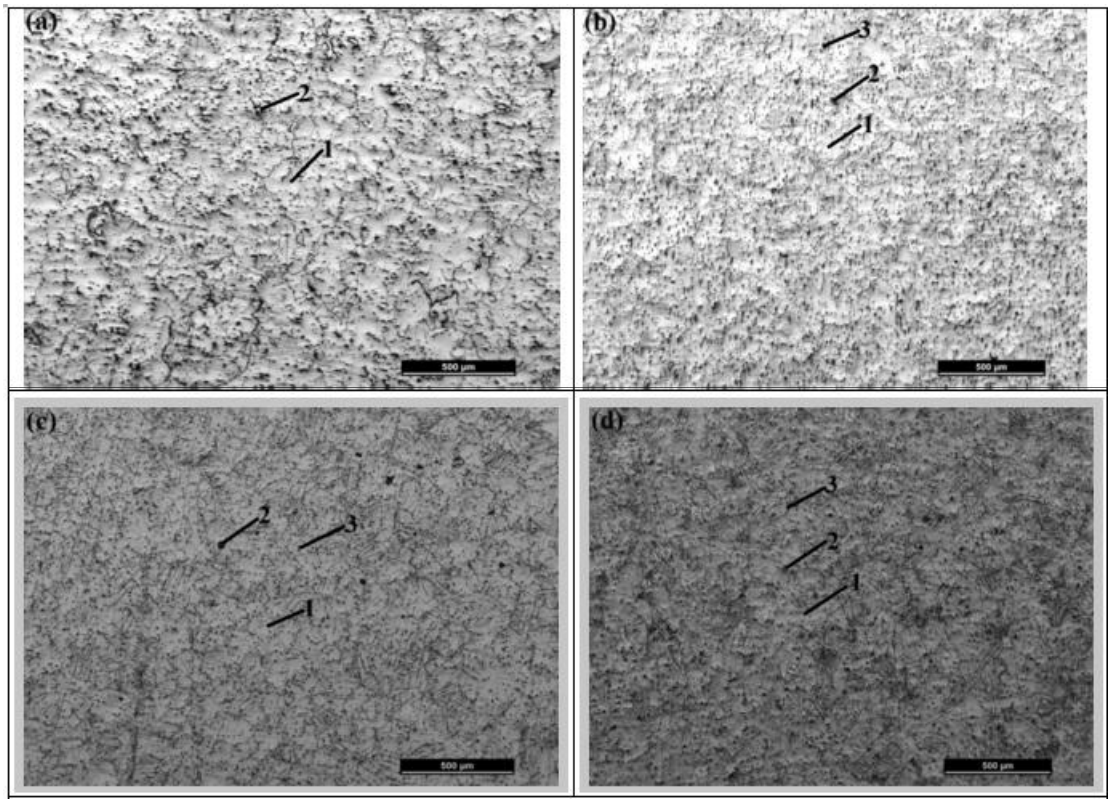

Figure 2: OM of (a) Mg-5Zn (b) Mg-5Zn-0.3Ca (c) Mg-5Zn-0.3Mn (d) Mg-5Zn-0.3Sr with legends (*1. α-Mg 2.$MgZn_2$ 3.Mg_x-$(Ca/Mn/Sr)_y$*)

4. Conclusion

Lattice strain and dislocation density rise, especially in the alloy containing Sr, while crystallite size gradually decreases in the order Mg–5Zn > Ca > Mn > Sr. From ~99 µm to ~76 µm, a distinct grain refinement trend is seen. In Mg–5Zn, the strengthening mechanism is matrix-dominated; in Ca, it is grain refinement; in Mn, it is combined grain and dislocation strengthening; and in Sr, it is grain, dislocation, and

precipitation strengthening. These results verify that Sr offers the best overall strengthening and microstructural refinement.

Acknowledgment
Mr Rajnish Kumar Bharati acknowledges the research fellowship received from National Institute of Technology, Jamshedpur and MHRD, India.

References

[1] M. Niinomi, Mechanical biocompatibilities of titanium alloys for biomedical applications, *Materials Science Forum* 539–543 (2007) 193–200. https://doi.org/10.4028/0-87849-428-6.193
[2] M.P. Staiger, A.M. Pietak, J. Huadmai, G. Dias, Magnesium and its alloys as orthopedic biomaterials: A review, *Biomaterials* 27 (2006) 1728–1734. https://doi.org/10.1016/j.biomaterials.2005.10.003
[3] J. Vormann, Magnesium: nutrition and metabolism, *Molecular Aspects of Medicine* 24 (2003) 27–37. https://doi.org/10.1016/S0098-2997(02)00089-4
[4] N.E.L. Saris, E. Mervaala, H. Karppanen, J.A. Khawaja, A. Lewenstam, Magnesium: an update on physiological, clinical and analytical aspects, *Clinica Chimica Acta* 294 (2000) 1–26. https://doi.org/10.1016/S0009-8981(99)00258-2
[5] T. Qi, J. Weng, F. Yu, W. Zhang, G. Li, H. Qin, Z. Tan, H. Zeng, Magnesium ions promote osteogenic differentiation and bone formation, *Biological Trace Element Research* (2020). https://doi.org/10.1007/s12011-020-02183-y
[6] P. Scherrer, Determination of the size and internal structure of colloidal particles by means of X-rays, *Nachrichten von der Gesellschaft der Wissenschaften zu Göttingen, Mathematisch-PhysikalischeKlasse*(1918) 98-100. https://doi.org/10.1002/andp.19183620404
[7] G.K. Williamson, W.H. Hall, X-ray line broadening from filed aluminium and wolfram, *Acta Metallurgica* 1 (1953) 22–31. https://doi.org/10.1016/0001-6160(53)90006-6
[8] G. K. Williamson, R.E. Smallman, Dislocation densities in some annealed and cold-worked metals from measurements on the X-ray Debye–Scherrer spectrum, *Philosophical Magazine* 1 (1956) 34–46. https://doi.org/10.1080/14786435608238074.

Figure Caption

Figure 1	XRD patterns of alloys Mg-5Zn, Mg-5Zn-0.3Ca, Mg-5Zn-0.3Mn, Mg-5Zn-0.3Sr.
Figure 2	OM of (a) Mg-5Zn (b) Mg-5Zn-0.3Ca (c) Mg-5Zn-0.3Mn (d) Mg-5Zn-0.3Sr with legends (*1. α-Mg 2.*$MgZn_2$ *3.*Mg_x*-(Ca/Mn/Sr)*$_y$)